Numerical Analysis of Torsional Behavior of Ultra-High Performance Fiber Reinforced Concrete

Jongbum Park, Sung-Yong Park, Keunhee Cho, Sung-Tae Kim, Kihyon Kwon, Changbin Joh

Researcher, Structural Engineering Research Institute, Korea Institute of Civil Engineering and Building Technology, Goyang-si, Gyeonggi-do, Korea

Research Fellow, Structural Engineering Research Institute, Korea Institute of Civil Engineering and Building Technology, Goyang-si, Gyeonggi-do, Korea

Senior Researcher, Structural Engineering Research Institute, Korea Institute of Civil Engineering and Building Technology, Goyang-si, Gyeonggi-do, Korea

Senior Researcher, Structural Engineering Research Institute, Korea Institute of Civil Engineering and Building Technology, Goyang-si, Gyeonggi-do, Korea

Senior Researcher, Structural Engineering Research Institute, Korea Institute of Civil Engineering and Building Technology, Goyang-si, Gyeonggi-do, Korea

Research Fellow, Structural Engineering Research Institute, Korea Institute of Civil Engineering and Building Technology, Goyang-si, Gyeonggi-do, Korea

ABSTRACT: Numerous tests on the material level and structure level are necessary for the development of the analysis process and design guideline of concrete. For ultra-high performance fiber reinforced concrete (UHPFRC), the tensile characteristics must be considered because these characteristics vary significantly due to the diverse ranges of fiber type and fiber volume fraction. The testing of large structural members for the development of the structural analysis and design procedure can be reduced by limiting the number of material and structure tests and by adopting numerical analysis methods like finite element analysis. The established numerical models can be applied to study the effects of geometry, loading state and reinforcement state of steel and fiber on the structural behavior. Experimental studies on the torsional behavior of UHPFRC are currently carried out but only a very few studies were dedicated to the numerical analysis. Accordingly, this study intends to propose and validate a numerical model for the analysis of the torsional behavior of large structural members made of UHPFRC. To that goal, the Cast Iron model of the FE software ANSYS is adopted to model the material behavior of UHPFRC and a numerical model is developed and validated by comparing the results to those of previous literature. Parametric study is implemented to examine the effect of the material parameters related to the tensile behavior and the Cast Iron model on the torsional behavior. The torsion-angle of twist behavior of UHPFRC box beams obtained by the numerical model reveals that the proposed model predicts satisfactorily the torsional behavior of UHPFRC box beams. This indicates that the Cast Iron model applying appropriate tension characteristics obtained through tensile test can be exploited to predict the overall torsion-angle of twist behavior of UHPFRC box beams.

KEYWORDS: Ultra-High Performance Fiber Reinforced Concrete (UHPFRC), Torsional Behavior, Tension Strain Hardening, Cast Iron Material Model.

I.INTRODUCTION

Ultra-High Performance Fiber Reinforced Concrete (UHPFRC), which has been recently the subject of active research, is a cementitious composite material featured by high strength, high toughness and high durability that can provide compressive strength higher than 150 MPa thanks to the development of tensile strain hardening through sufficient inclusion of fibers. Due to its high material cost and the need for advanced quality control skills, the application of UHPFRC remains limited (Singh et al. 2017).

Most of the studies on UHPFRC focus on the identification of its material characteristics. Wille et al. (2014) published a report arranging the strain hardening/softening characteristics of UHPFRC obtained through direct tensile test. Since the strain softening or strain hardening as well the ductility developed by UHPFRC vary according to the type and volume fraction of the fiber, these tensile characteristics are the most critical factors influencing the structural behavior of UHPFRC. Accordingly, the number of analytical and experimental studies on the flexural behavior of UHPFRC considering these tensile characteristics is restlessly growing (Yang et al. 2010, Yang et al. 2011). On the other hand, theoretical and experimental studies on the torsional behavior of UHPFRC are rare (Yang et al. 2013, Kwahk et al. 2015), and the absence of numerical studies by finite element analysis is noteworthy.

In concern with the numerical analysis of the flexural behavior of UHPFRC or fiber reinforced concrete (FRC), studies can be distinguished as those using sectional analysis method to derive the load-deflection relation (Yoo & Choo 2016, Yoo & Yoon 2015, Ferrier et al. 2012) and those using finite element (FE) analysis (Singh et al. 2017, Özcan et al. 2009). The studies using section analysis predict the behavior for unidirectional flexure and cannot be applied for the torsional behavior. Singh et al. (2017) performed the numerical analysis of UHPFRC using the concrete damaged plasticity (CDP) model of the FE software ABAQUS but did not consider the torsional behavior. Özcan et al. (2009) conducted FE analysis of steel fiber reinforced concrete beams using the SOLID65 element of the FE software ANSYS. However, the SOLID65 element assumes linear model for the tensile stress-strain relation and cannot simulate the tensile strain hardening of UHPFRC since the post-cracking tensile stress is not supported.

The present study suggests a numerical model applying the Cast Iron material model of the FE software ANSYS[11] to simulate the tensile characteristics of UHPFRC and analyzes the resulting torsional behavior. The proposed numerical model is validated by comparing the results to those of previous literature. Finally, parametric study is implemented to examine the effect of the tensile characteristics of UHPFRC on its torsional behavior.

II. TORSIONAL SPECIMENS

The UHPC box beam specimens of Kwahk et al. (2015) are analyzed by FE model and the results are compared. The test members present box section with dimensions of $350 \times 350 \times 3,000$ mm and were fabricated with the details shown in Fig. 1. The material properties and test variables are listed in Table 1[6]. The main variables are the tensile strength and elastic modulus of concrete, the quantity of fiber, and the amount of longitudinal and transverse reinforcement. The torsion test is conducted by fixing one end of the specimen and by applying a torque on the other hand so as to measure the torsion-angle of twist behavior. The behavioral comparison of Specimen 1 and Specimen 2 shows the influence of the cross-sectional area of the longitudinal reinforcement, the comparison of Specimen 2 and Specimen 3 shows the influence of the stirrup spacing, and the comparison of Specimen 1 and Specimen 4 shows the influence of the fiber volume fraction. Finite element analysis is performed for four specimens without prestressing and the results are compared to the experimental values.
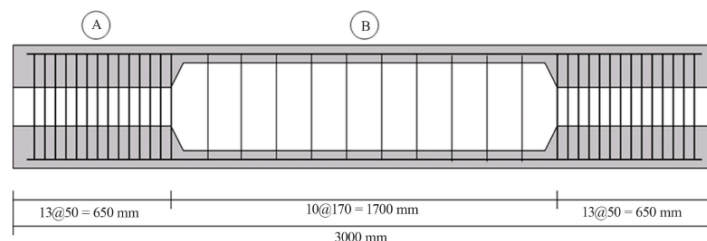
(a) Side elevation view of beam specimen
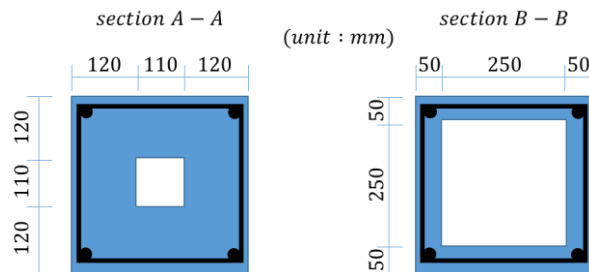
(b) Cross sections of beam specimen

Fig. 1 Details of UHPFRC box beam specimen

Table 1 Test beam material properties and experimental parameters [6]

No.	SPECIMEN	Steel fiber (%)		Steel reinforcement		Stirrup spacing	Crack initiation strength (f_{cr})	Tensile strength (f_t)
		16.5mm	19.2mm	stirrup	Longitudinal			
1	SH-P0-F1.5-L1-S1(D13)	0.5	1	D10	D13@4	5@340	8.23	11.48
2	SH-P0-F1.5-L1-S1(D10)	0.5	1	D10	D10@4	5@340	8.23	11.48
3	SH-P0-F1.5-L1-S2	0.5	1	D10	D10@4	10@170	7.77	11.18
4	SH-P0-F1-L1-S1	0.5	0.5	D10	D13@4	5@340	6.96	8.39

III. FINITE ELEMENT MODEL

The nonlinear FE analysis program ANSYS 13.0 is used for the analysis of the torsional behavior of the UHPFRC beams. UHPFRC is modeled using the Cast Iron material model and the 8-node brick element (SOLID185) so as to comprehend the different stress-strain curves in tension and compression. The SOLID65 element generally used to model concrete material in ANSYS enables to simulate the compressive failure and the tensile cracking of concrete but assumes zero for the post-cracking stiffness (stress) as shown in Fig. 2(a). In the analysis, the convergence is secured with regard to the sudden stress change considering some residual post-cracking stress until a definite strain. As shown in Fig. 2(b), this model is inappropriate in simulating the tensile strain hardening of UHPFRC in which the post-cracking tensile stress continues to increase until the tensile strength.

The Cast Iron Plasticity model was originally developed for gray cast iron [11]. The micro-structure of gray cast iron shown in Fig. 3[11] reveals a two-phase material with graphite flakes inserted in the steel matrix, and induces different behaviors in tension and compression. In tension, cracks are formed due to the graphite flakes and the material becomes brittle at low strength. In compression, the graphite flakes behave as incompressible medium transferring the stress and the steel matrix governs the overall behavior. This model exhibits isotropic elasticity with the same elastic behavior in tension and compression. As shown in Fig. 4[11], the yield strength and the isotropic hardening behavior differ in tension and compression, and present different yield criteria and plastic flow potentials. The tensile behavior is influenced by pressure and adopts the Rankine maximum stress criterion. The compressive behavior does not depend on the pressure and uses the von Mises yield criterion. Fig. 5[11] presents the yield surfaces of cast iron for tension and compression.

(a) Tensile stress-strain curve of   Solid65 Element   (b) Tensile stress-tensile strain curve of UHPFRC
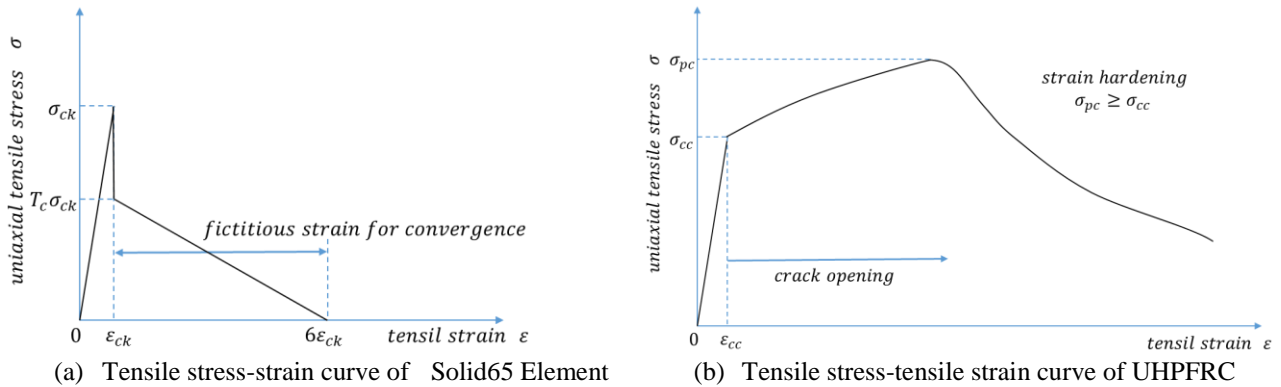
Fig. 2Tensile stress-strain curve
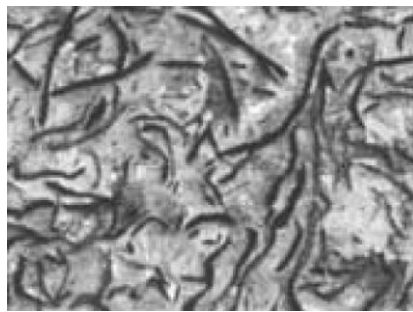
Fig. 3Graphite flakes in steel matrix [11]
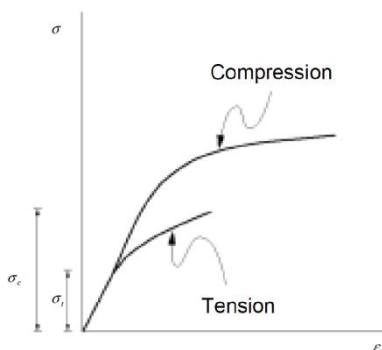
Fig. 4 Stress-strain curve in tension and compression at
Cast Iron Plasticity Model [11]
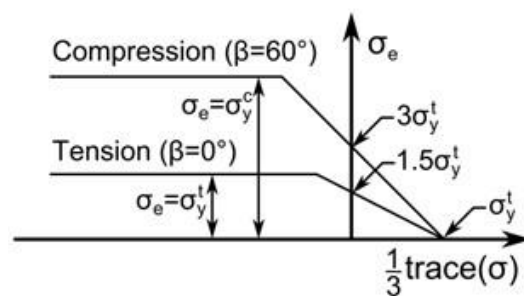
Fig. 5Cast iron yield surfaces for compression and
tension [11]

In this model, the plastic Poisson's ratio (v^{pl}) considered additionally to the stress-strain curve determines the volumetric expansion in occurrence of tensile plastic deformation. When its value of 0.5 and there is no plastic volumetric change, the von Mises flow potential is applied.

As explained above, the Cast Iron material model was developed for gray cast iron but this model can appropriately simulate the characteristics of UHPFRC for which the tensile stress increases in case of hardening in the tensile behavior, and the tensile and compressive behaviors differ.

Accordingly, UHPFRC is modeled by Cast Iron material and SOLID185 elements in this study. The plastic Poisson's ratio is set to 0.2 identically to the elastic ratio of UHPFRC. The longitudinal and transverse reinforcement are modeled

using the 3-dimensional truss model LINK180 Element, and elastic-perfect plastic model is adopted as material characteristics.

As shown in Fig. 6 and expressed in Equations (1) to (4), the compressive stress-strain curve of UHPFRC can be modeled linearly up to the compressive strength as done by Yoo & Choo(2016) and the tensile stress-strain curve can be drawn as proposed by Yoo & Yoon (2015) assuming polylinear tension strain hardening curves complying with AFGC/SETRA recommendation and the Guideline of Fiber Reinforced SUPER Concrete (KCI 2017).

$$\varepsilon_c = \frac{f_c}{E_c} \tag{1}$$

$$\varepsilon_{cr} = \frac{f_{cr}}{E_c} \tag{2}$$

$$\varepsilon_u = \varepsilon_c + \frac{w_u}{L_{eq}} \tag{3}$$

$$\varepsilon_{lim} = \varepsilon_c + \frac{w_{lim}}{L_{eq}} \tag{4}$$

where E_c is the elastic modulus; f_c is the compressive strength; ε_c is the compressive strain at f_c;f_{cr} is the crack initiation strength;ε_{cr} is the compressive strain at f_{cr};f_t is the tensile strength;ε_u is the tensile strain at f_t;and, ε_{lim} is the tensile strain when there is no tensile stress anymore.Here, $w_u = 0.3$ mm;$w_{lim} = 5.3$ mm;and, the characteristic length $L_{eq} = \frac{2}{3}h$ with h being the depth of the beam.
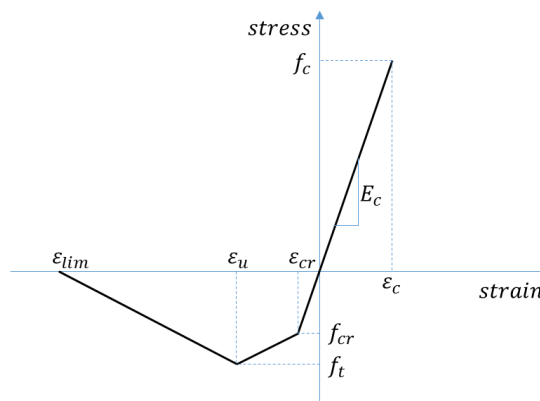
Fig. 6 Stress-strain curve of UHPFRC

IV. ANALYSIS RESULTS

The four types of UHPFRC box beam specimens of Kwahk et al.(2015) were analyzed using the cast iron material model and the 8-node reduced integration brick element(SOLID185 Element). As shown in Fig. 1, the 650 mm-long sections at the extremities have thickness of 120 mm and are thicker than the thickness of 50 mm at the center. Therefore, these end sections indicated in red in Fig. 7(a) are modeled as linear elastic material with the elastic modulus of UHPFRC, and are modeled with the 50 mm-thickness of the central section indicated in green. Fig. 7(b) shows the boundary conditions and the analytic meshing of UHPFRC and steel reinforcement. The left-side end is fixed and the end point of the right one is let free to displace so as to apply the torsion load. Since both ends (indicated in red in Fig. 7(a)) are modeled as linear elastic, the central section (indicated in green in Fig. 7(a)) can develop uniform torsion. The

experimental value of the elastic modulus being 45 GPa, all the specimens are assumed to have elastic modulus of 45 GPa and the other physical properties are those listed in Table 1 for the FE analysis.

Fig. 9(a) presents the torsional moment-angle of twist curves of specimen SH-P0-F1.5-L1-S1 obtained by FE analysis together with the experimental values. Sets of two specimens were fabricated for each test variable and are distinguished by the values -1 and -2 at the end of the legends as SH-P0-F1.5-L1-S1-1 and SH-P0-F1.5-L1-S1-2.

The results of FE analysis are indicated by pred.1 and show that the torsional moment at the initiation of cracking of UHPFRC and the peak torsional moment are predicted with fair accuracy. However, the angle of twist at the torsional strength appears under-evaluated by the analysis compared to the experiment. In order to find the reason for this difference, the torsional stiffness of the box beam section calculated by considering only UHPFRC without the steel reinforcement was obtained and the theoretical value of the torsional moment-angle of twist obtained using the torsional stiffness in the elastic region is indicated in Fig. 9(a). In the figure, the comparison of the theoretical value G*Ip with the analytic value shows that the analysis result is slightly stiffer. Considering that the theoretical value ignored the steel reinforcement, this means that the FE analysis provides valid results.

(a) Material properties input

(b) View of mesh and boundary conditions
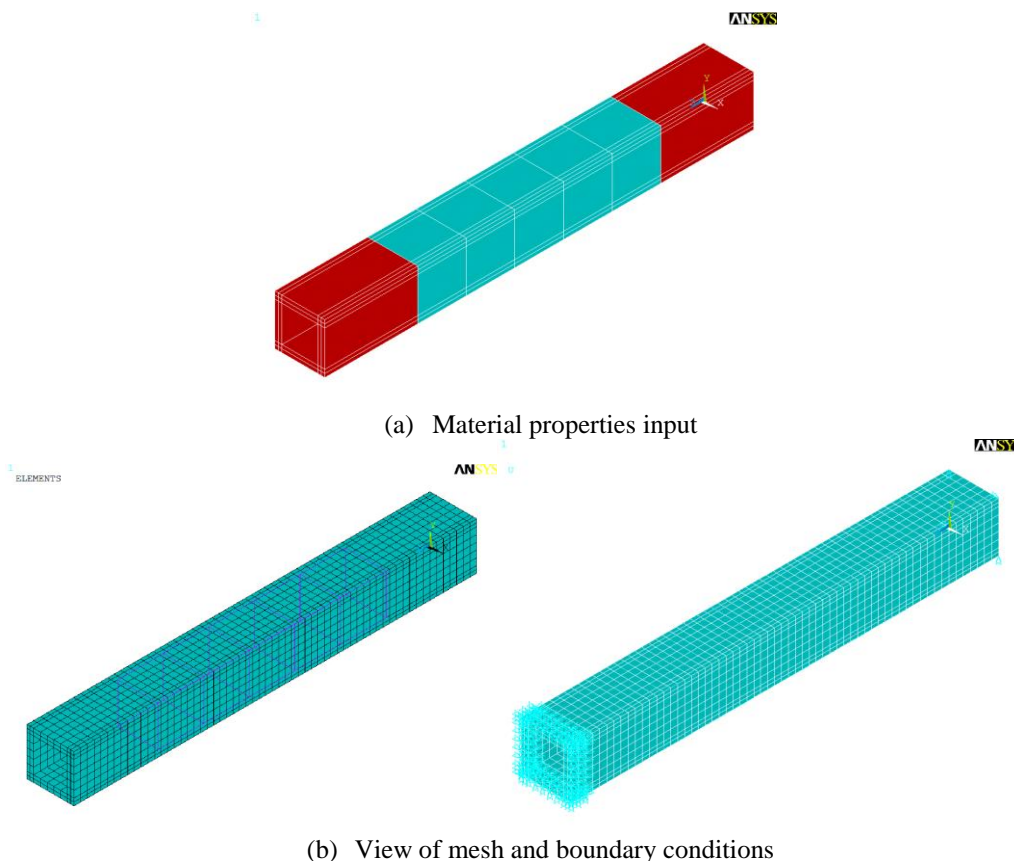
Fig. 7 Modeling of UHPFRC box beam

Consequently, the difference between the experimental and analytical values in this study can be attributed to the actual occurrence of some deformation at the fixed end in the experiment. Assuming zero deformation at the fixed end in the test, the twist angle (α) can be converted as follows using Equation (5) by measuring the vertical displacement d at the location L (1.6 m) far away from the fixed end.

$$\alpha = \frac{d}{r}\frac{1}{L} \tag{5}$$

where r is half the height of the box beam.

As shown in Fig. 8, if in the experiments the occurrence of a twist angle is assumed at the fixed end and if the distance L' to a fictitious support is set to 3.2 m that is twice the distance L, the experimental value can be seen to have doubled the twist angle, which means that the analytical twist angle has doubled and can be compared to the experimental results. As in Fig. 9(a), the analytic values indicated by pred.2 denote those for which the twist angle analyzed has been doubled and are seen to agree well with the experimental values. This validates the estimated distance proposed between the fictitious support and the fixed end.

The torsion moment-twist angle curves of the other three specimens were analyzed by the same method and the results are drawn in Figs. 9(b) to (d). The analyzed curves agree generally well to the experimental results and the peak torsional moment given by the analysis for all the specimens is also seen to fit accurately to the experimental values. Table 2 compares the peak torsional moments obtained experimentally with those predicted by the proposed numerical model. For three types of specimen with 1.5% of steel fiber, the predicted values approach the experimental ones up to 94.7% to 116.7%, and for the specimen with 1.0% of steel fiber, the predictions are seen to be slightly smaller to be within 86.1% to 95.7% of the test values. This observation is due to (1) adopting the smeared model of the tensile characteristics of UHPFRC in the FE analysis of the whole structure; and (2) the presence of material uncertainty in the actual structure.
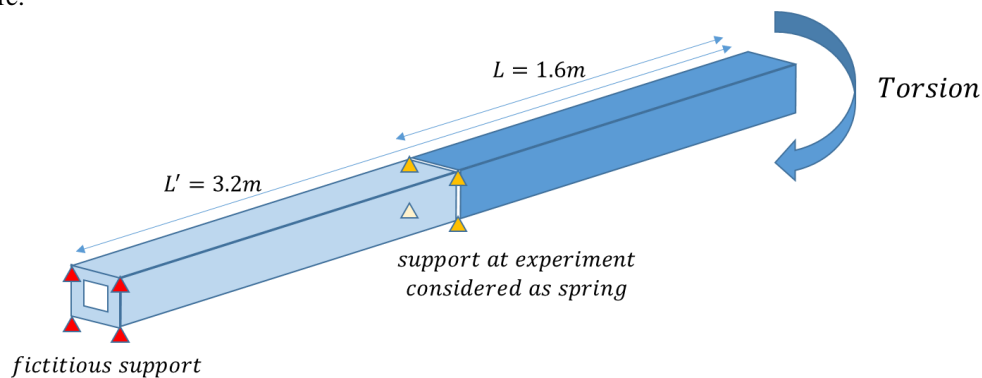
Fig. 8 Assumption for support condition at the test
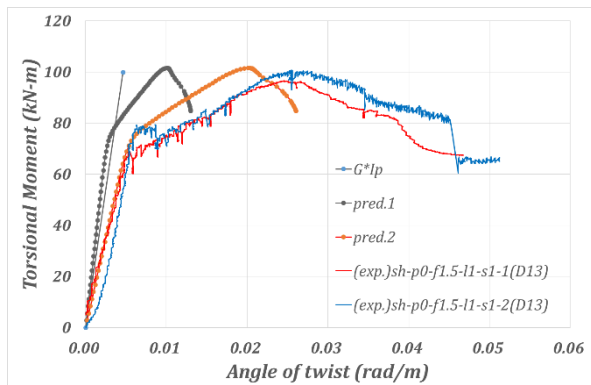
(a) SH-P0-F1.5-L1-S1(D13)
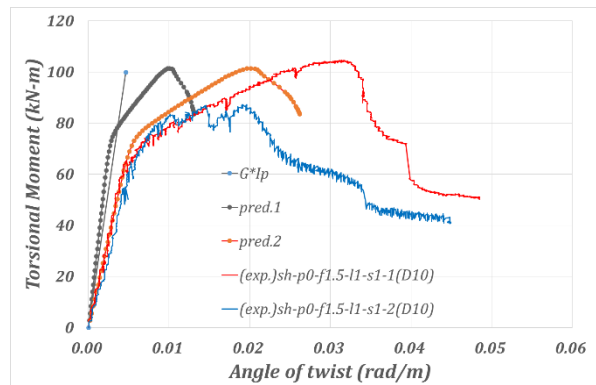
(b) SH-P0-F1.5-L1-S1(D10)
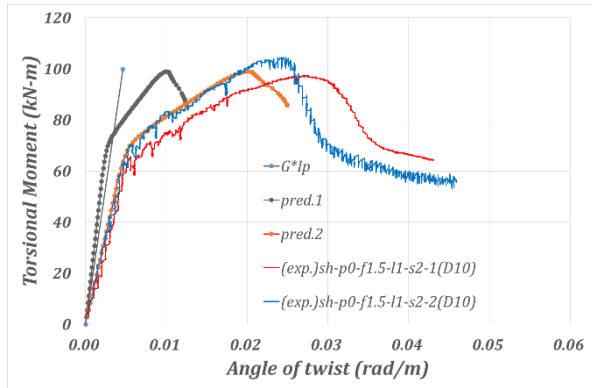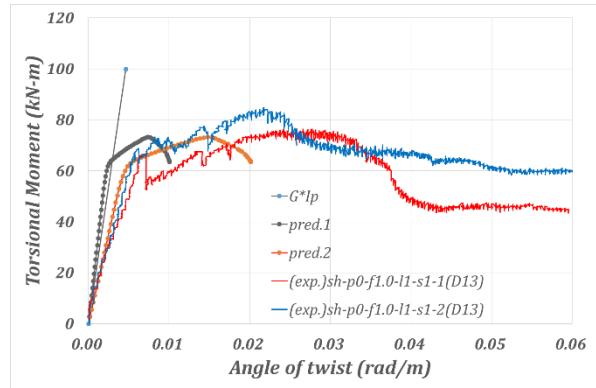
(c) SH-P0-F1.5-L1-S2   (d) SH-P0-F1.0-L1-S1

Fig. 9 Torsion-twist angle curves of UHPFRC box beams

Table 2 Comparison of experimental and predicted ultimate torsional moment

No.	Specimen	Experiment (kN-m)		Predicted (kN-m)	Pred./Exp. (%)	
		1	2		1	2
1	SH-P0-F1.5-L1-S1(D13)	96.6	100.7	102.0	105.6%	101.3%
2	SH-P0-F1.5-L1-S1(D10)	104.6	87.2	101.8	97.3%	116.7%
3	SH-P0-F1.5-L1-S2	97.5	104.6	99.1	101.6%	94.7%
4	SH-P0-F1-L1-S1	76.4	84.9	73.1	95.7%	86.1%

Fig. 10 plots the deformed shape, the von Mises stresses and strains at the peak torsional moment and at the failure. It shows that in the numerical analyses, deformation increases in overall section and then small region goes to the failure like the experimental results.
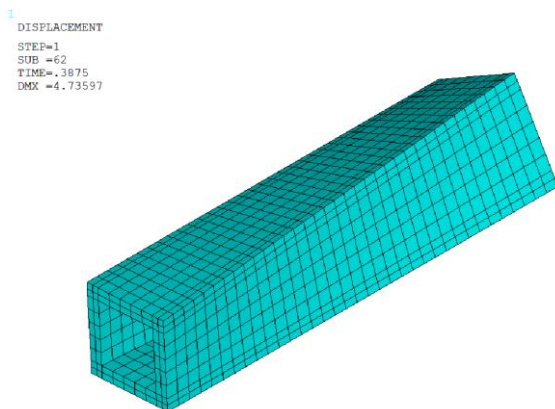
(a) Deformed shape at the peak torsional moment   (b) Deformed shape at the failure
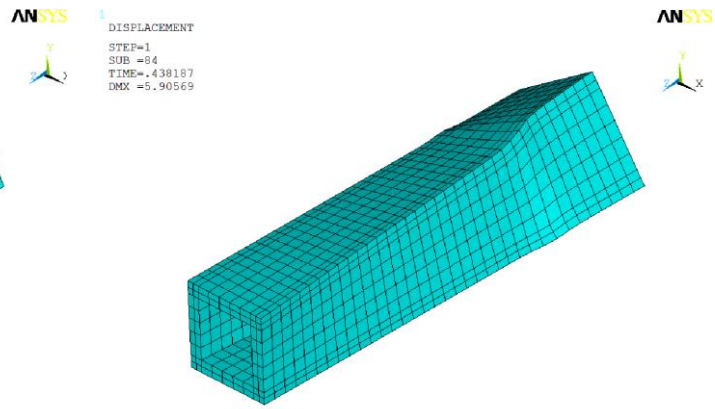
(c) Von Mises strain at the peak torsional moment

(d) Von Mises strain at the failure

(e) Von Mises stress at the peak torsional moment

(f) Von Mises stress at the failure
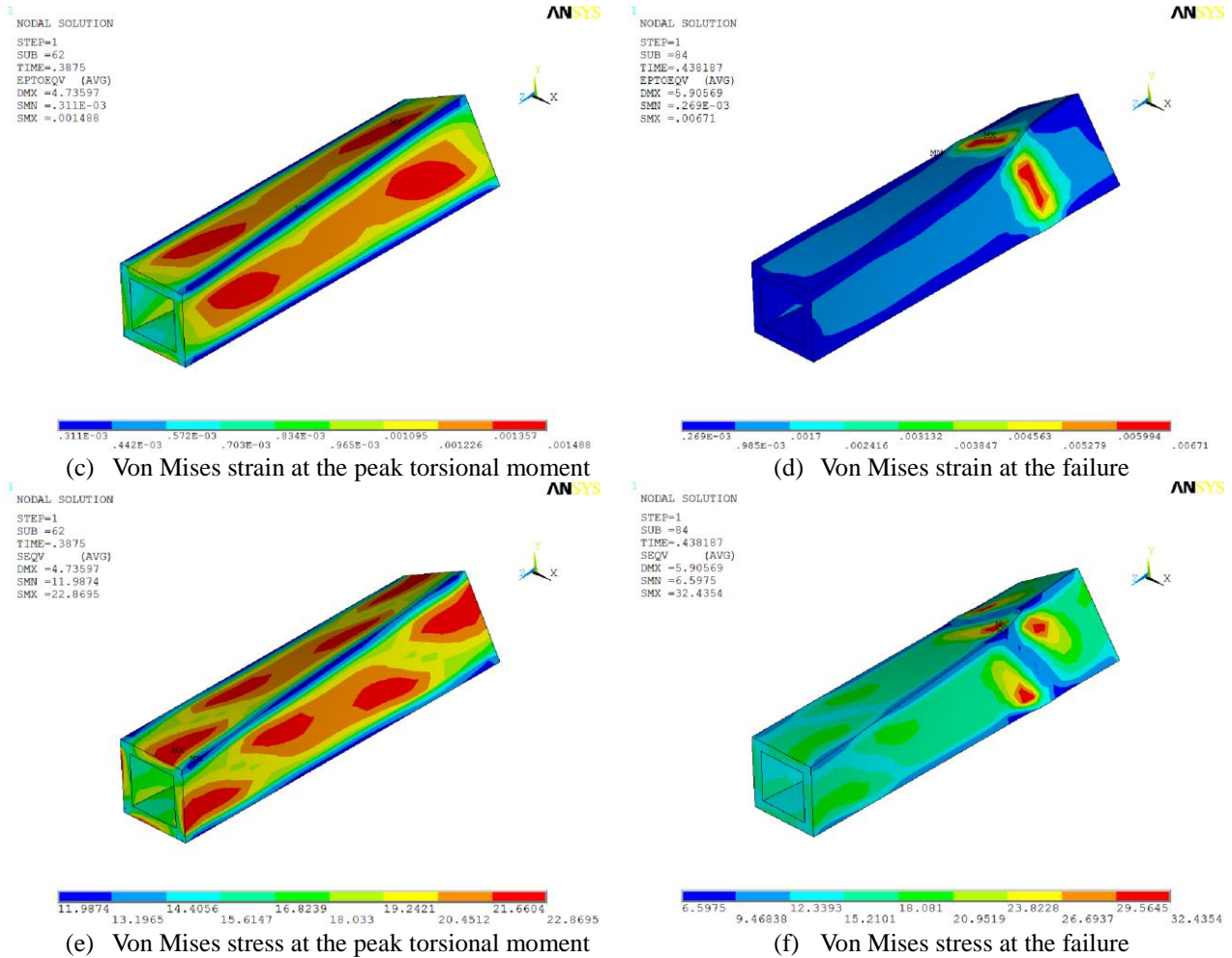
Fig. 10 Results of FE analysis

V. PARAMETRIC STUDY

The effect of w_u and w_{lim} representing the tensile characteristics of UHPFRC is analyzed. Fig. 11 arranges the results of the analysis of the torsional behavior by parametric study with the variables in Table 3. It shows that the polylinear tension strain hardening curves representing the tensile characteristics can be obtained by inverse analysis of the torsional test results.

Fig. 12 presents the analytic torsional behavior obtained by considering the plastic Poisson's ratio (v^{pl}) of the Cast Iron model as variable with the values in Table 4. The figure indicates that the plastic Poisson's ratio mainly influences the peak torsional moment by reducing the peak torsional moment as the ratio increases.

Table 3 Parametric variables for tensile properties of UHPFRC

Case	w_u	w_{lim}
Cast 1 (Origin)	0.3 mm	5.3 mm
Case 2	0.6 mm	5.3 mm
Case 3	0.3 mm	10.6 mm
Case 4	0.6 mm	10.6 mm

Table 4 Parametric variables for plastic Poisson's ratio of Cast Iron Model

Case	v^{pl}
Case A	0.1
Case B (Origin)	0.2
Case C	0.3
Case D	0.4
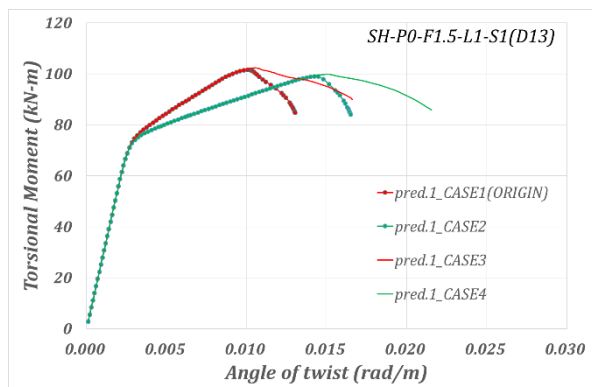
Fig. 11 Torsion-twist angle curves according to tensile properties
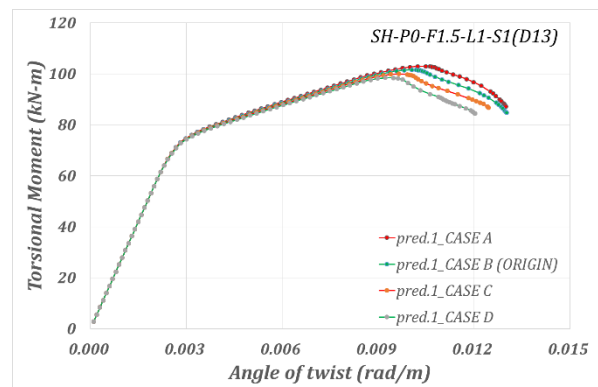
Fig. 12 Torsion-twist angle curves according to plastic Poisson's ratio

VI.CONCLUSION

A numerical model applying the Cast Iron material model of the FE software ANSYS was developed to predict the torsional behavior of UHPFRC box beam. The Cast Iron model was chosen owing to the possibility to simulate the compressive and tensile behaviors of UHPFRC. The adopted material properties were those proposed in previous literature. The FE analysis results obtained in the present study were validated by comparing them with the results of previous torsion tests. The torsional strength of the UHPFRC box beam provided by the analysis using the proposed numerical model predicted the experimental values with error within 16%, and the Cast iron model could predict the ultimate torsional strength of the UHPFRC box beam with good accuracy. In addition, the torsional moment-twist angle curves obtained numerically by FE analysis were in good agreement with the experimental values of the four types of beams when the support conditions were appropriately considered. Moreover, parametric study was also conducted to examine the torsional behavior according to the tensile properties of UHPFRC. It appeared that the actual torsional behavior could be fairly well simulated by appropriate calibration of the variables representing the tensile characteristics of UHPFRC. This indicates that the Cast Iron model applying appropriate tension characteristics obtained through tensile test can be exploited to predict the overall torsional behavior of UHPFRC box beams.

REFERENCES

[1] Singh, M., Sheikh, A. H., Ali, M. M., Visintin, P., & Griffith, M. C. (2017). Experimental and numerical study of the flexural behaviour of ultra-high performance fibre reinforced concrete beams. Construction and Building Materials, 138, 12-25.

[2] Wille, K., El-Tawil, S., & Naaman, A. E. (2014). Properties of strain hardening ultra high performance fiber reinforced concrete (UHP-FRC) under direct tensile loading. Cement and Concrete Composites, 48, 53-66.

[3] Yang, I. H., Joh, C., & Kim, B. S. (2010). Structural behavior of ultra high performance concrete beams subjected to bending. Engineering Structures, 32(11), 3478-3487.

[4] Yang, I. H., Joh, C., & Kim, B. S. (2011). Flexural strength of large-scale ultra high performance concrete prestressed T-beams. Canadian Journal of Civil Engineering, 38(11), 1185-1195.

[5] Yang, I. H., Joh, C., Lee, J. W., & Kim, B. S. (2013). Torsional behavior of ultra-high performance concrete squared beams. Engineering Structures, 56, 372-383.

[6] Kwahk, I., Joh, C., & Lee, J. W. (2015). Torsional Behavior Design of UHPC Box Beams Based on Thin-Walled Tube Theory. Engineering, 7(03), 101.

[7] Yoo, S. W., & Choo, J. F. (2016). Evaluation of the flexural behavior of composite beam with inverted-T steel girder and steel fiber reinforced ultra high performance concrete slab. Engineering Structures, 118, 1-15.

[8] Yoo, D. Y., & Yoon, Y. S. (2015). Structural performance of ultra-high-performance concrete beams with different steel fibers. Engineering Structures, 102, 409-423.

[9] Ferrier, E., Labossière, P., & Neale, K. W. (2012). Modelling the bending behaviour of a new hybrid glulam beam reinforced with FRP and ultra-high-performance concrete. Applied Mathematical Modelling, 36(8), 3883-3902.

[10] Özcan, D. M., Bayraktar, A., Şahin, A., Haktanir, T., & Türker, T. (2009). Experimental and finite element analysis on the steel fiber-reinforced concrete (SFRC) beams ultimate behavior. Construction and Building Materials, 23(2), 1064-1077.

[11] ANSYS, Mechanical APDL version 15, Canonsberg (PA): ANSYS Inc. (2013).

[12] Korea Concrete Institute (KCI), Guideline of Fiber Reinforced SUPER Concrete (2017).